AIP | Review of Scientific Instruments

A collimated neutron detector for RFP plasmas in MST

W. J. Capecchi, J. K. Anderson, P. J. Bonofiglo, J. Kim, and S. Sears

Citation: Review of Scientific Instruments **87**, 11D826 (2016); doi: 10.1063/1.4961304
View online: http://dx.doi.org/10.1063/1.4961304
View Table of Contents: http://scitation.aip.org/content/aip/journal/rsi/87/11?ver=pdfcov
Published by the AIP Publishing

A collimated neutron detector for RFP plasmas in MST

W. J. Capecchi,[a] J. K. Anderson, P. J. Bonofiglo, J. Kim, and S. Sears
University of Wisconsin- Madison, Madison, Wisconsin 53706, USA

(Presented 7 June 2016; received 9 June 2016; accepted 25 July 2016;
published online 23 August 2016)

The neutron emissivity profile in the Madison Symmetric Torus is being reconstructed through the use of a collimated neutron detector. A scintillator-photomultiplier tube (PMT) system is employed to detect the fusion neutrons with the plasma viewing volume defined by a 55 cm deep, 5 cm diameter aperture. Effective detection of neutrons from the viewing volume is achieved through neutron moderation using 1300 lbs of high density polyethylene shielding, which modeling predicts attenuates the penetrating flux by a factor of 10^4 or more. A broad spectrum of gamma radiation is also present due to the unconfined fusion proton bombardment of the thick aluminum vacuum vessel. A 15 cm cylindrical liquid scintillator of 3.8 cm diameter is used to further increase directional sensitivity. A fast (5 ns rise time) preamplifier and digitization at 500 MHz prevent pulse pile-up even at high count rates ($\sim 10^4$/s). The entire neutron camera system is situated on an adjustable inclining base which provides the differing plasma viewing volumes necessary for reconstruction of the neutron emissivity profile. This profile, directly related to the fast-ion population, allows for an investigation of the critical fast-ion pressure gradient required to destabilize a neutral beam driven Alfvénic mode which has been shown to transport fast ions. *Published by AIP Publishing.* [http://dx.doi.org/10.1063/1.4961304]

I. INTRODUCTION

Fast-ion confinement in magnetically confined plasma is essential for achieving burning conditions through self-heating. A common component of plasmas, fast ions are generated either through external RF heating, fusion reactions, or neutral beam injection. Neutron diagnostics become available to assist in diagnosing fast-particle dynamics when considering deuterium fast-ions interacting with a deuterium plasma. Neutron camera systems have been implemented on other devices such as MAST,[1] TFTR,[2] and JET[3] to study fast-ion dynamics, though never in the reversed field pinch (RFP) configuration. The Madison Symmetric Torus (MST), with the relatively low magnetic field of an RFP, has naturally high beta and large shear, providing an interesting environment in which to study fast-ion physics.

In MST, typical plasmas (I_p = 200-500 kA, B = 0.2-0.5 T) along with a 1 MW, 25 keV deuterium neutral beam injector (NBI) provide a 2.45 MeV neutron flux from the d(d,n)^{3}He reaction that is dominated by beam-target fusion. This allows for the neutron emissivity to be correlated to the fast-ion density via

$$\Gamma_{MST} \cong \Gamma_{bt} = \iint f_{fi}(r,E)\, n_i \sigma v_{fi} dV\, dE \qquad (1)$$

where Γ_{MST} is the total MST neutron flux, n_i the ion density, σv_{fi} the fusion reactivity evaluated at the fast ion energy, and f_{fi} is the fast-ion distribution function. Large populations of fast-ions develop in the core of MST due to their near-classical confinement,[4] with classical modeling predicting fast-ion density up to 20% of the bulk density. The beam injects super-Alfvénic ions into the plasma which can destabilize Alfvén eigenmodes and trigger rapid fast-ion transport.[5] In addition, an energetic-particle mode (EPM) driven by the fast-ion pressure gradient has been identified which overcomes the Alfvén continuum damping due to the strong particle drive. This mode appears as abrupt ($\sim$100 μs) bursts of magnetic activity and causes a rapid drop in fast-ion content and appears to create an upper limit on fast-ion beta in MST.

A collimated adjustable neutron detector (CiNDe) has been constructed for MST to measure the fast-ion density profile and may expose a critical fast-ion pressure gradient that destabilizes the EPM.

II. CiNDe Design

The detector specifications (time and energy response) and the shielding providing the collimation are both key aspects of the design. A spatially resolved neutron emission measurement requires insensitivity to neutrons originating outside the region of interest and to other forms of radiation. Although a compact directional neutron detector is feasible for the detection of D-T fusion neutrons with minimal to no shielding through the use of scintillating fibers,[6] the lower energy of MST's D-D fusion neutrons makes this approach untenable. Collimation is instead achieved using large amount of moderating shielding. High energy neutrons react with matter primarily through elastic scattering, transferring energy most effectively to low-Z materials like high density polyethylene (HDPE) and paraffin wax which have high hydrogen content. The large initial energy of the neutrons still requires large amounts of shielding to effectively moderate the neutrons. Thus CiNDe is constructed using a combination of HDPE and

Note: Contributed paper, published as part of the Proceedings of the 21st Topical Conference on High-Temperature Plasma Diagnostics, Madison, Wisconsin, USA, June 2016.
[a]capecchi@wisc.edu

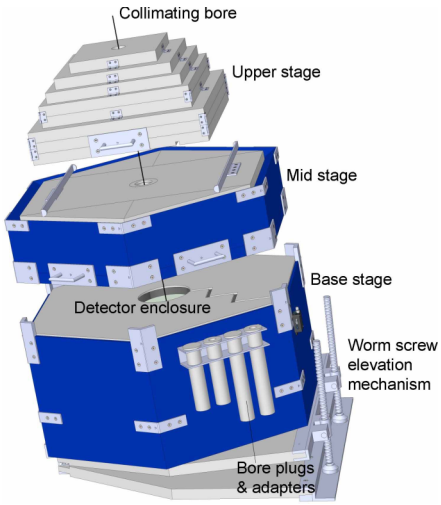

FIG. 1. CAD model of the collimated neutron detector (CiNDe). HDPE provides neutron shielding and a long bore into the bottom stage, housing the detector, determines the plasma viewing volume.

paraffin totaling over 1300 lbs and a minimum thickness of 46 cm.

Due to the weight and mobility requirement, CiNDe is composed of three detachable stages (see Fig. 1) of HDPE material. The base can be positioned and the upper two stages added and secured for measurements. The lowest stage is constructed from an array of cylinders, the gaps of which are filled with paraffin wax. The central cylinder was removed and a copper sheath inserted, allowing for the detector assembly to be placed into the central void. The cylindrical array is mounted on a baseplate consisting of two 3.8 cm slabs hinged on one side. The side opposite to the hinge features a dual worm-screw jack worked in unison via a chain drive which allows the entire apparatus to be inclined up to ~15°. By adjusting the inclination of the camera to adjust the plasma viewing volume and ensembling over many similar dishcarges, a neutron emissivity profile can then be reconstructed and normalized against an absolutely calibrated total MST flux neutron detector.

Modeling of the neutron energy spectrum through HDPE shielding with MCNP[7] reveals the expected behavior; as neutrons penetrate more deeply into the shielding, a decreasing percentage remains at full energy and those that have scattered have an increasing probability of scattering again and more often, resulting in pile-up at the lowest energy (Fig. 2). This shows that for 15 in. shielding (less that the minimum thickness of CiNDe shielding), transmission is reduced by 99.83%. The targeted viewing volume is defined by placing the detector assembly at the bottom of a single long bore through the three stages. The depth (55 cm) and bore diameter (5 cm) define a 1.6° cone half angle with an 8 cm width at the MST midplane. This provides adequate spatial resolution based on classical estimates of profile shape from the transport analysis code TRANSP.[8]

Due to the equal branching of D-D fusion, this measurement takes place in the presence of a strong gamma background. The d(d,p)t branch creates a 3.02 MeV proton which is unconfined in the low magnetic field of MST, strikes the aluminum vessel wall, and emits a shower of gammas with typical energies around 1 MeV.[9] Neutrons do not interact with

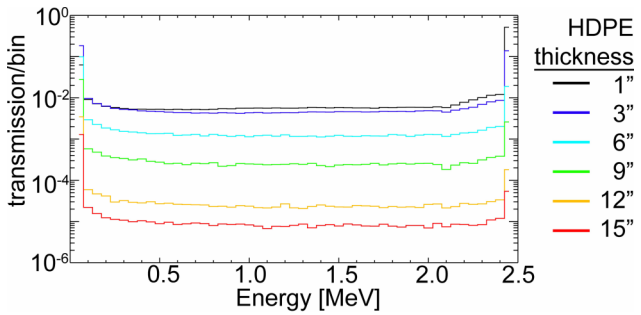

FIG. 2. MCNP modeling of neutron energy distribution through HDPE shielding.

the aluminum except by elastic scatter, meaning that they are relatively unaffected, though slightly diffused, by their transit through the vessel wall. Although HDPE provides modest shielding to gammas, the primary shielding is through a set of thick rectangular cross section toroids that surround the scintillator with at least 13 cm of lead. Despite the large amounts of shielding present, a large background signal remains. The methodology developed to cope with background is discussed in Section III.

The neutron detector is a scintillator-PMT type. The scintillator is a Saint-Gobain BC-501A liquid MAB cell which detects neutrons via proton-recoil. The fluorescent molecule anthracene has peak emission at 425 nm which is well coupled to the R580 Hamamatsu PMT which has a peak response at 420 nm. The anode current from the PMT is then amplified and converted to a voltage pulse by a TIA60 Thorlabs preamplifier with a gain of 3×10^5 V/A. The signal is then digitized at 500 MHz in order to facilitate post-processing of the pulse shapes. The scintillator was designed with two purposes in mind. First, the cell dimensions were chosen within physical space limitations to optimize detection of signal neutrons while minimizing detection of shield-penetrating neutrons. A 15 cm × 3.8 cm diameter cylindrical geometry was chosen, giving a ~2.55× suppression of the shield-penetrating neutron signal level. The second reason this scintillator was chosen was that small differences exist between neutron and gamma pulse shapes due to how the fluorescent molecule excites due to each type of interaction. By analyzing these small differences, gammas can be identified and filtered out of the background radiation signal. Initial measurements presented here do not incorporate any background reduction by pulse shape discrimination. Analysis of data indicates a very subtle difference in recorded pulse shapes, and normal laboratory noise on the signal has blurred any clear speciation. Improved techniques may aid in future analyses; here we collect a meaningful collimated signal by removing the measured background signal through differencing techniques.

III. INITIAL RESULTS

Data has been collected for the first reconstruction of the fast-ion beta profile in MST. A lead slug, 5 cm × 5 cm diameter, was inserted into the bore, situated in front of the detector in order to filter out the direct gamma radiation. Additionally, HDPE bore plugs were used to gather a large dataset of background signal, and a 7.6 cm HDPE spacer was placed

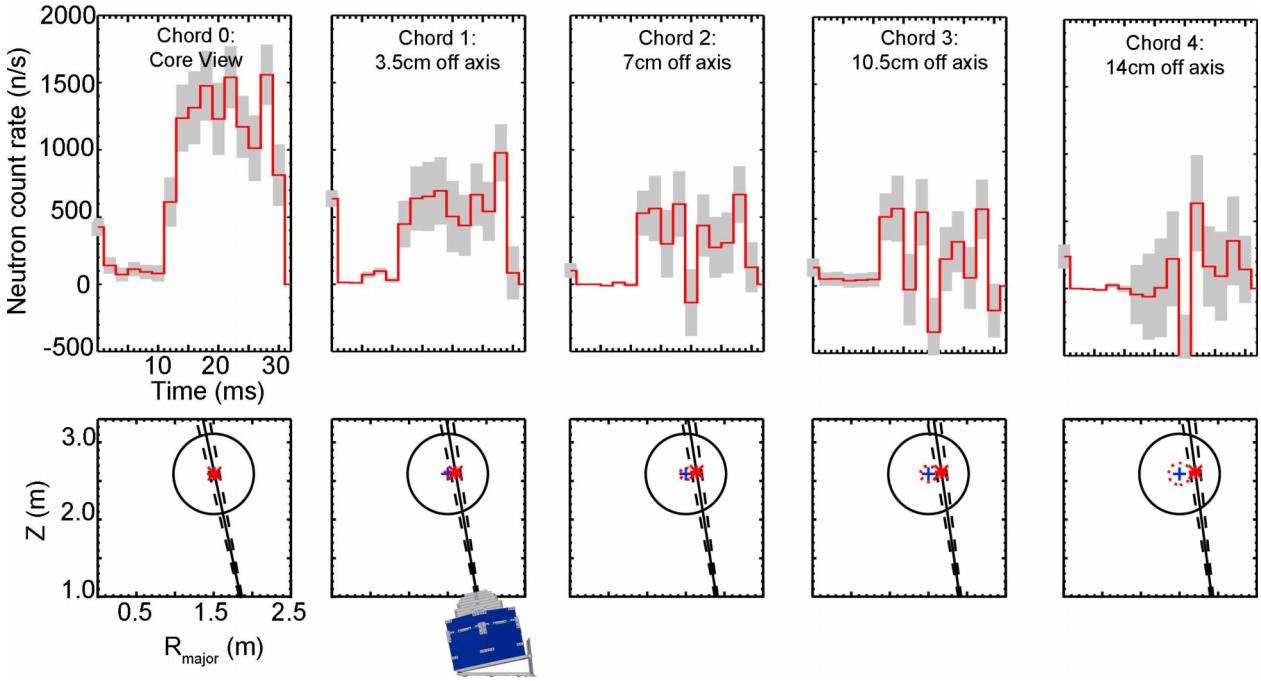

FIG. 3. Neutron count rate for five viewing chords. The neutron signal decreases with distance from the core and is effectively zero at an impact parameter of 14 cm. CiNDe orientation (to scale) shows poloidal cross section of viewing volume for each associated neutron data above.

behind the detector to decrease the likelihood of neutron backscatter affecting the measurement. Open- and closed-bore datasets were collected with plasma conditions of 300 kA, a reversal parameter of F = 0 ($B_T = 0$ at the wall), and a density of $n_e \approx 1e13\,\mathrm{cm}^{-3}$. The neutral beam, running at 40 A, 25 keV, with full deuterium fuel, is between 10 and 35 ms. This presents both a well diagnosed set of plasma conditions to compare with previous experiments and conditions where the m = 1, n = 5 EPM is commonly observed. The open- and closed-bore datasets were then compared in order to ascertain the net neutron count rate. The background count rate was properly scaled to account for slight global emissivity differences between the two datasets. Removal of the large background signal leads to substantial uncertainty, but a clear neutron emissivity localization in the core has been measured, as shown in Figure 3.

The measured neutron rate is plotted as a function of time for five different chord views through the plasma. From left to right, the CiNDe tilt angle is adjusted to give discrete views with impact parameters of 0, 3.5, 7, 10.5, and 14 cm. The signal decreases with radius and is effectively zero at the impact parameter of 14 cm. This is consistent with a core localized fast-ion population that is peaked in the core resulting in decreasing chord signals at increasingly off-core viewing angles. These data provide the information necessary to reconstruct a 2D poloidal neutron emission profile. As the fusion product is proportional to the fast-ion density, this is the first direct measure of NBI-born fast-ion density profile shape in the RFP configuration.

IV. DISCUSSION

The analysis of an initial small dataset has shown the capability of utilizing a collimated neutron detector to determine the fast-ion density profile in MST. Incorporating the energy dependence of a classically slowing fast-ion distribution will give a measure of local fast ion pressure and beta. Increased numbers of chords each with larger datasets will improve the statistical significance of the results. Further investigation into different plasma conditions will probe the MST phase space to determine the critical fast-ion beta gradient required to destabilize EPMs as well as set an upper limit of an achievable MST fast-ion beta.

SUPPLEMENTARY MATERIAL

See supplementary material for the data presented in Figure 2 showing the transmitted neutron energy spectrum through polyethylene and in Figure 3 depicting the neutron count rate for five CiNDe viewing chords.

ACKNOWLEDGMENTS

This material is based upon work supported by the U.S. Department of Energy Office of Science, Office of Fusion Energy Sciences program under Award No. DE-FC02-05ER54814.

[1]M. Cecconello *et al.*, Rev. Sci. Instrum. **81**, 10D315 (2010).
[2]A. L. Roquemore *et al.*, Rev. Sci. Instrum. **61**, 3163 (1990).
[3]O. N. Jarvis *et al.*, Fusion Eng. Des. **34-35**, 59 (1997).
[4]J. K. Anderson *et al.*, Plasma Phys. Controlled Fusion **56**, 094006 (2014).
[5]L. Lin *et al.*, Phys. Plasmas **21**, 056104 (2014).
[6]G. A. Wurden *et al.*, Rev. Sci. Instrum. **66**, 901 (1995).
[7]See http://mcnp-green.lanl.gov/s for MCNP.
[8]R. Goldston *et al.*, J. Comput. Phys. **43**, 61 (1981).
[9]C. L. Fink *et al.*, Nucl. Instrum. Methods Phys. Res., Sect. A **505**, 5 (2003).